
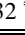





## TENSILE PROPERTIES OF PURE PLA POLYMER DEDICATED FOR ADDITIVE MANUFACTURING


### ZATEZNA SVOJSTVA ČISTOG PLA POLIMERA ZA ADITIVNU PROIZVODNJU

Originalni naučni rad / Original scientific paper  
Rad primljen / Paper received: 17.10.2024  
<https://doi.org/10.69644/ivk-2024-03-0263>

Adresa autora / Author's address:

<sup>1)</sup> Innovation Centre of the Faculty of Mechanical Eng., Belgrade, Serbia A. Milovanović  0000-0003-4668-8800; M. Milošević  0000-0002-2418-1032 \*email: [amilovanovic@mas.bg.ac.rs](mailto:amilovanovic@mas.bg.ac.rs)

<sup>2)</sup> University of Belgrade, Faculty of Mechanical Engineering, Belgrade, Serbia A. Sedmak  0000-0002-5438-1895; M. Paunić  0000-0002-4180-9813; M. Popović  0000-0003-3607-9243

<sup>3)</sup> University Union- Nikola Tesla, Faculty of Information Technology and Engineering, Belgrade, Serbia A. Mitrović  0000-0002-5183-6276

<sup>4)</sup> The Academy of Applied Technical Studies, Belgrade, Serbia

#### Keywords

- additive manufacturing
- fused deposition modelling
- PLA
- tensile properties
- FEM analysis

#### Abstract

*This research aims to provide comprehensive data on PLA polymer tensile properties via conducted tensile tests on 100 % infill density specimens (for 0.3; 0.2; 0.1 mm layer height), and all possible lower infill results (i.e., from 90 to 10 %, with a 10 % increment) obtained by interpolation of previous research findings. Tensile tests are performed using dedicated ISO 527-2 standard. Next, the FEM analysis is performed for the 100 % case to verify the FEM model. Thus, the implemented constitutive models of this thermoplastic material and FEM simulations match the experimental data.*

#### INTRODUCTION

Additive Manufacturing (AM) is a convenient ‘new’ technology for producing prototypes and functional parts, housing many different sub-technologies for fabricating final components, /1/. The most used materials in AM are polymers and metals. One of the most utilized sub-technologies for component fabrication is Fused Deposition Modelling (FDM) technology, where the material is melted right before being deposited onto a build platform /2/. For this particular case, the most suitable materials are thermoplastics, such as PLA (PolyLactic Acid), ABS (Acrylonitrile Butadiene Styrene), PET (PolyEthylene Terephthalate), PP (PolyPropylene), etc. /3/.

This research focuses on PLA, which has several advantages over other FDM thermoplastic materials. For example, PLA holds one of the highest stiffness values and high flexural strength for a thermoplastic material, with ultimate tensile strength (UTS) ranging from 38 to 48 MPa. The literature findings from the last two decades have reported the immense potential for improvement in PLA’s physical and mechanical properties, indicating the material’s potential in various fields, /4-6/. Additionally, PLA can be easily extruded into filament shape without significant energy or time inputs, making it an inexpensive and readily available FDM material. Recyclability is also an advantage here since it can be easily moulded and reshaped after AM use through

#### Ključne reči

- aditivna proizvodnja
- modeliranje deponovanjem topljenog materijala
- PLA
- zatezna svojstva
- MKE analiza

#### Izvod

*Cilj istraživanja je pružanje celovite slike o zateznim svojstvima materijala na osnovu eksperimenata na uzorcima sa 100 % ispunom (za 0.3; 0.2; 0.1 mm visine sloja) i sve ostale količine ispune (od 90 do 10 %, sa inkrementom 10 %), dobijeno interpolacijom rezultata iz prethodnih istraživanja. Zatezanje je rađeno prema ISO 527-2 standardu. Zatim se sa MKE analizira 100 % ispuna, radi verifikacije MKE modela. Time je pokazano da korišćeni konstitutivni modeli ovog termoplastičnog materijala i same MKE simulacije odgovaraju eksperimentalnim podacima.*

processes such as extrusion and injection moulding. One interesting advantage of this material is its proven biocompatibility, suitable for food packaging, and utilization in the biomedical field, /3, 4/.

As a raw material, PLA is transparent, stable at low temperatures, with modest oxygen and water permeability, and high grease and oil resistance /5/. However, PLA properties vary with changes in molecular weight. An increase in molecular weight results in higher tensile strength and shear viscosity due to chain entanglement and length but decreases crystallinity, /6/.

A distinctive advantage of PLA over other petrochemical polymers is its material feature (variable stereochemistry) that allows for significant alterations in its properties, /7/. In such a way, the PLA can be in both semicrystalline and amorphous form. The mechanical properties and biodegradation rate of PLA are contingent upon its chemical structure. Furthermore, PLA can be plasticized to enhance its crystallinity by blending it with other polymers such as starch, citrate ester, polyethylene glycol, sorbitol, and oligomeric lactic acid, /8/.

Concerning FDM, the mechanical properties of finished components highly depend on utilized process parameters, such as layer height, infill density, pattern, and both build and raster orientation, /9-11/. In /9/ a comprehensive insight into the influence of infill density on PLA’s tensile properties

is shown. The research was conducted on tensile specimens from 90 % to 10 %, with an increment of 10 % on 13 different infill patterns. Worth pointing out is that honeycomb infill is overall the most useful pattern in terms of mechanical properties and has proven itself in many functional applications, /12-13/.

This research aims to use the data from conducted tensile tests on 100 % infill density specimens with honeycomb infill structure to interpolate it with 90-10 % data from /9/. In this way, the full influence of infill density on this particular material is obtained. As an addition, this research will also include FEM simulations for tensile cases and will show fitting of numerical predictions with experimental results.

## MATERIALS AND METHODS

The tensile specimen geometry used here follows the recommendations for type 1A design from ISO 527-2:2012 standard. The chosen specimen geometry is suitable for an axial extensometer with a 50 mm measuring range. The specimen's engineering drawing is shown in Fig. 1. The CAD model was prepared in SolidWorks® (Dassault Systèmes, Vélizy-Villacoublay, France) and later loaded to the slicer software (Simplify3D) using STL file format. Specimens are manufactured using PLA material on an FDM machine with main process parameters shown in Table 1. The top and bottom layers are manufactured with a 'rectilinear' raster

orientation and a honeycomb infill structure. A visual interpretation of 'rectilinear' raster orientation is given in Fig. 2, from /11/. The pure PLA material supplied for this research is so-called 'silk-grey' from the German RepRap company (InnovatiQ GmbH, Kapellenstraße, Feldkirchen, Germany).

This research focuses on tensile specimens with 100 % infill, which are divided into three groups according to layer height, i.e., 0.3, 0.2, and 0.1 mm. The specimen groups here consist of seven specimens each, for a more thorough result analysis. An additional set of three specimen groups with 90 % infill is prepared to patch our 100 % results with the results from /9/, to interpolate elastic modulus (E) and UTS values for all other infill densities. Hence, the 90 % groups consist of just three specimens. In this manner, the research will show the tensile results for pure PLA material used in FDM, from 100 % to 10 % infill density (with an increment of 10 %).

Thus, the 100 and 90 % specimens have a honeycomb infill structure (see Fig. 2a), available in the Simplify3D® software, and the geometrically closest infill pattern from /9/ to the one used here is the so-called 'Tri-Hexagon' infill (see Fig. 2b). The reason why we have different infill patterns is the fact that these two research papers use different slicer software, but the overall similarity between these two patterns is sufficient.

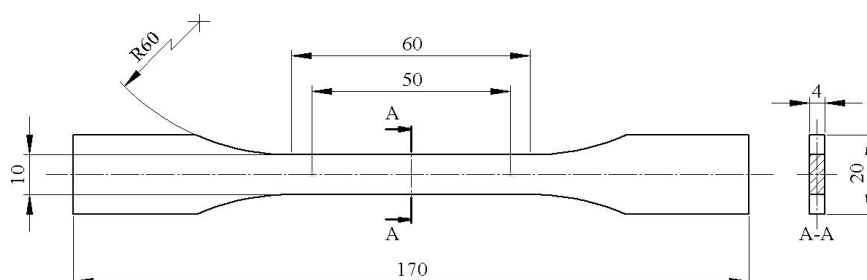


Figure 1. Tensile specimen engineering drawing, according to ISO 527-2:2012, type 1A (units in mm).

Table 1. Main FDM process parameters.

Filament diameter [mm]	Nozzle diameter [mm]	Nozzle temperature [°C]	Build platform Temperature [°C]	Nozzle speed [mm/s]	Raster orientation	Infill pattern
1.75	0.4	200	60	40	Rectilinear	Honeycomb

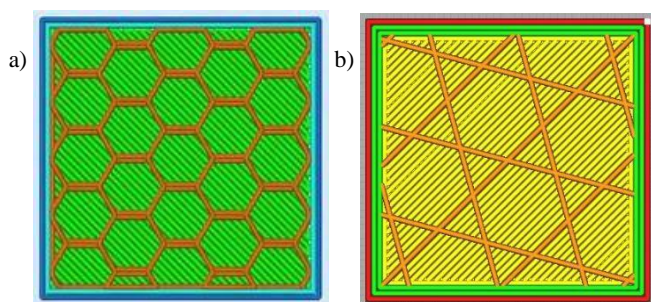


Figure 2. Infill patterns: a) honeycomb; b) tri-hexagon.

Tensile tests are performed on the Shimadzu AGS-X machine (Shimadzu Corp., Kyoto, Japan) equipped with a 100 kN load cell, paired with an Epsilon axial extensometer (Epsilon Tech. Corp, Jackson, WY, USA), model 3542 (see Fig. 3). The used extensometer is certified for polymer testing according to ISO 527-2 standard, based on the descrip



Figure 3. Tensile specimen after the test.

tion on their website, /16/. The testing speed is 1 mm/min, according to the standard.

Next, the FEM simulations in Abaqus® CAE (Dassault Systèmes, Vélizy-Villacoublay, France) are performed for 100 % specimens and the PLA's constitutive model is created with the help of the 'Mcalibration' software tool (Ansys Inc., Canonsburg, PA, USA).

To create a proper constitutive model for PLA, for all three considered layer heights, additional sets of tensile specimens are prepared for higher velocity testing (i.e., 10 mm/min), and also compressive specimens for testing until fracture and for obtaining 25 % loops, performed similarly as in /17/. For simplicity, the data from these tests are considered for only representative specimens from three tested in each condition. Here, the stress-strain diagrams are shown only for higher velocity tensile tests.

This comprehensive analysis is suitable for an estimation of the plane-strain state near the crack tip for fracture toughness value calculations /14, 15/. Next, an accurate FEM model can be verified from tensile tests via good fitting of numerical simulation outputs with experimental results. Both previously mentioned actions are necessary for the authors' further research.

## RESULTS AND DISCUSSION

Engineering stress-strain responses from all three 100 % infill test groups are presented in Fig. 4. Here, it is visible that result repeatability is sufficient. Also, the diagrams have marked UTS for every specimen. Figure 5 contains average curves. MATLAB® software (Math Works, Natick, MA, USA) is employed to visualize the results and create average curves. For averaging, the full stress-strain response is considered, requiring equalization of data arrays from all seven specimens.

From Fig. 5, it is visible that the 0.3 mm curve has a slightly lower stiffness and UTS than the other two. The UTS here is around 42 MPa. The 0.2 mm and 0.1 mm average curves have similar stiffness which is visually obvious. Also, the failure strain is similar. However, the two differ in UTS, with values around 44 and 46 MPa for 0.2 mm and 0.1 mm layer cases, respectively. The brittle nature of PLA is clear from the images, as failure occurred at, or immediately after reaching UTS. The UTS and E values from /9/ are presented in Table 2. Tables 3 and 4 contain UTS and E data for the considered PLA material, respectively. The 100 % and 90 % data are obtained from tests, and the other values are interpolated following Table 2. From Tables 3 and 4 it is clear that high infill density increases both UTS and E values.

Next, the tensile specimens with 100 % infill are also tested at 10 mm/min crosshead speed. This will be useful when calibrating the PLA constitutive model in the 'MCalibration' software, for all three (layer) cases. The average curves from 'high-speed' tests are presented in Fig. 6.

When comparing average curves for 1 mm/min and 10 mm/min cases (see Figs. 5 and 6), one can see that with higher testing velocities, the stiffness (i.e., E) and UTS are higher, but the overall strain is lower. The UTS and E results for 10 mm/min are shown in Table 5. The greatest

improvement in properties from the 1 mm/min results is in the 0.3 mm case. The UTS value difference for the 10 mm/min loading case in 0.2 mm and 0.1 mm is below 1 MPa. Also, the stiffness value difference here is around 20 MPa, similar to the 1 mm/min case.

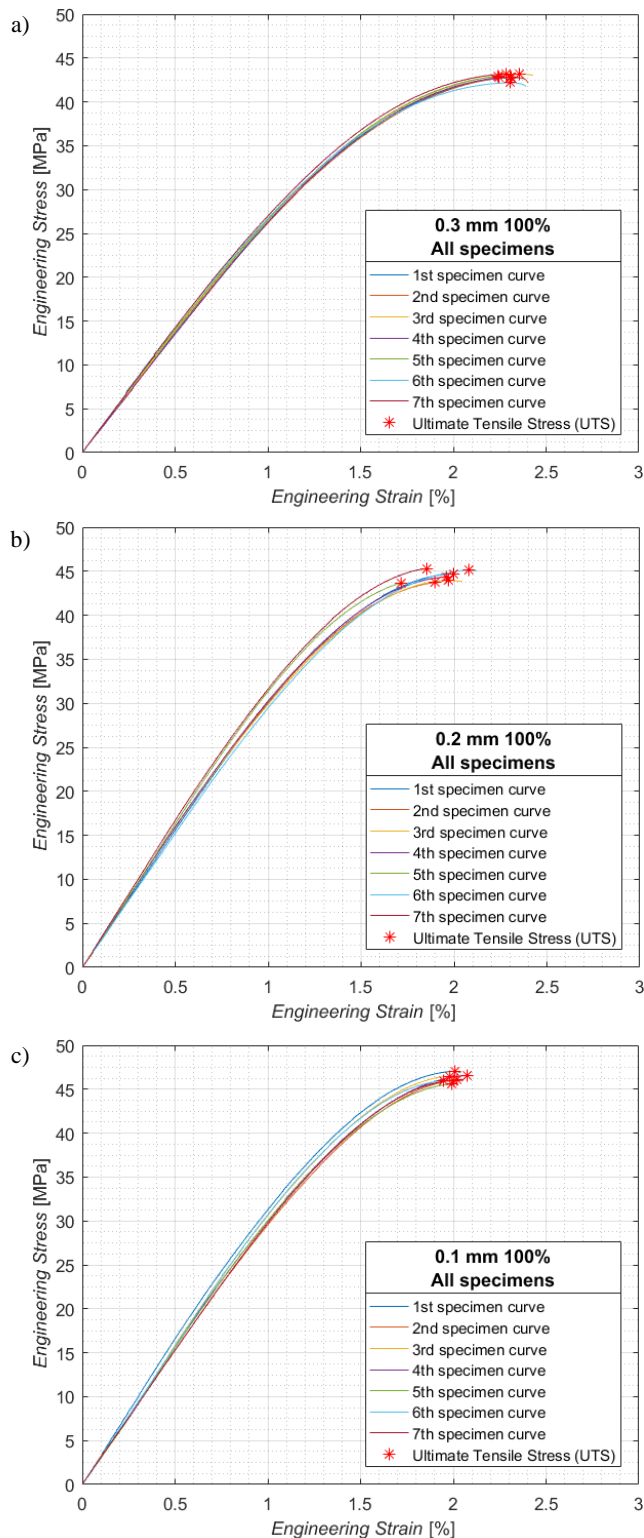


Figure 4. Engineering stress-strain results for: a) 0.3 mm specimen group; b) 0.2 mm specimen group; c) 0.1 mm specimen group.

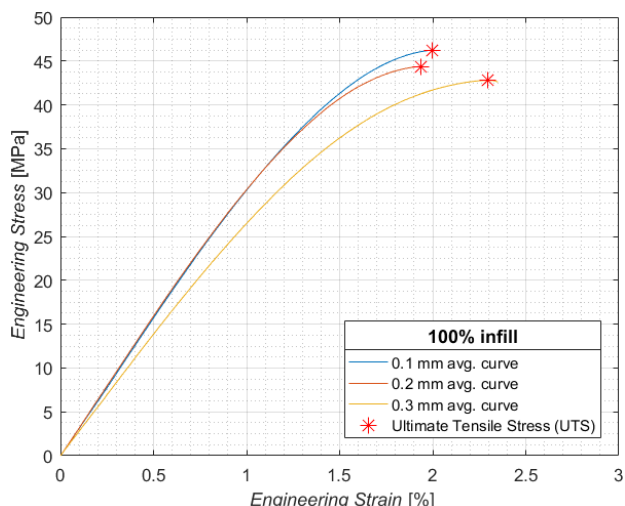


Figure 5. Average engineering stress-strain results by groups.

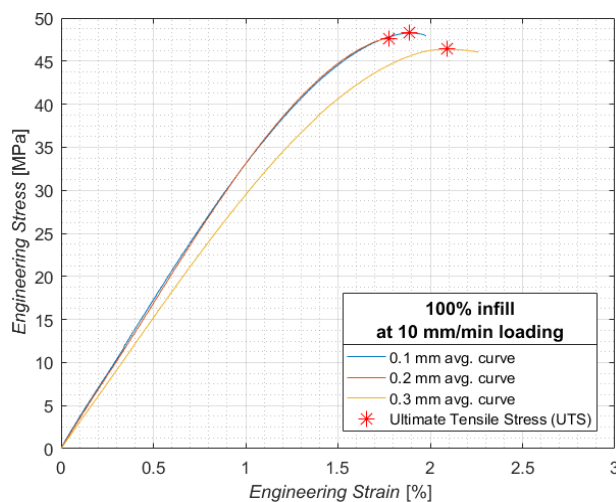


Figure 6. Average stress-strain data for 10 mm/min loading.

Table 2. The UTS and E values for the Tri-Hexagon infill pattern, extracted from /9/.

PLA	90%	80%	70%	60%	50%	40%	30%	20%	10%
UTS [MPa]	22.8	21.9	21.6	19.7	18.5	18.3	16.6	16.0	15.4
E [MPa]	2099.9	1988.8	1919.9	1777.7	1684.5	1594.2	1480.1	1413.8	1336.3

Table 3. The UTS values for all layer heights and infill densities (1 mm/min loading speed cases).

UTS [MPa]	100%	90%	80%	70%	60%	50%	40%	30%	20%	10%
0.3 mm	42.8	40.2	38.8	38.2	34.8	32.7	32.4	29.3	28.3	27.2
0.2 mm	44.3	41.7	40.2	39.7	36.1	34.0	33.6	30.4	29.3	28.2
0.1 mm	46.2	43.5	42.0	41.4	37.7	35.5	35.1	31.8	30.6	29.5

Table 4. The Elastic modulus (E) values for all layer heights and infill densities (1 mm/min loading speed cases).

E [MPa]	100%	90%	80%	70%	60%	50%	40%	30%	20%	10%
0.3 mm	2779.4	2600.0	2462.4	2377.2	2201.1	2085.6	1973.9	1832.6	1750.4	1654.5
0.2 mm	3197.5	2976.6	2819.1	2721.5	2519.9	2387.7	2259.8	2098.0	2004.0	1894.1
0.1 mm	3179.9	2995.0	2836.5	2738.3	2535.5	2402.5	2273.8	2111.0	2016.4	1905.9

Table 5. UTS and E values for 10 mm/min cases.

100% infill	0.3 mm	0.2 mm	0.1 mm
UTS [MPa]	46.3	47.6	48.2
E [MPa]	3004.0	3368.2	3389.6

The next step involves MCalibration software for PLA’s constitutive model creation. Unlike metals, thermoplastic behaviour is more difficult to explain due to material viscoplasticity and time/temperature-dependent behaviour, /18-20/. For simplicity, only room temperature is considered here. Fortunately, there are automatic calibration tools available that use tensile and compressive data of the material to adequately fit the proper constitutive model for FEM analysis, like the mentioned MCalibration software. Hence, the 100 % infill tensile results with 1 and 10 mm/min loading speed are utilized for this matter. In addition, to create a more precise FEM model, a set of 100 % compressive specimens are used for testing until failure and to create 25 % loops. The ‘Three-Network’ material model from the PolyUMod® library (see MCalibration software) is applied, which should provide the best fitting with our results, /21/.

To improve material model accuracy, the data is segmented into parts until 0.1, 0.2, 0.5, 1, 1.5, and 2 % deformation to gradually feed the software with the necessary data. In this way, the predictions have an R<sup>2</sup>-value of approx. 0.999 for all layer height cases. Next, the created PLA constitutive models are used in Abaqus CAE software to verify the FEM model.

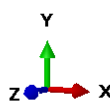
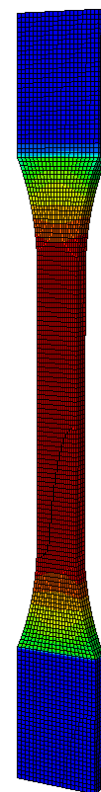
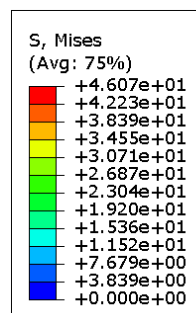


Figure 7. Tensile test simulation layout in Abaqus CAE software.

The tensile test simulation layout is presented in Fig. 7 (deformed shape). The lower portion of the specimen is fixed in the FEM simulation, and the upper portion is allowed to have vertical movement to best resemble the experiments. A highly refined mesh with 20-node quadratic hexahedral elements (C3D20R) with reduced integration, is used on the specimen, resulting in 13760 elements and 68057 nodes.

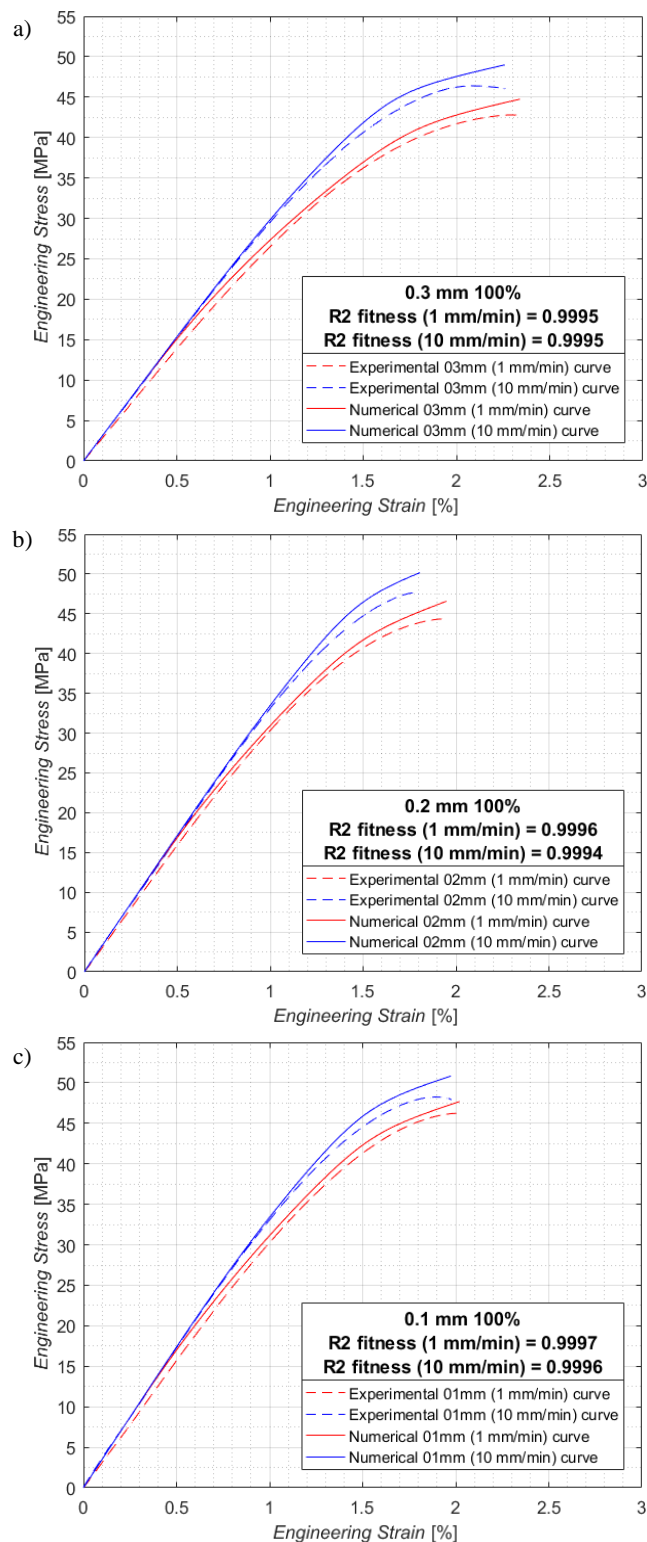


Figure 8. Experimental and numerical fitting of stress-strain response: a) 0.3 mm case; b) 0.2 mm case; c) 0.1 mm case.

The stress-strain outputs from FEM simulations are exported and compared with experimental data. The final R<sup>2</sup>-value fitness of numerical data is above 0.999 for all layer height cases, in both 1 and 10 mm/min testing speeds, thereby, proving a very good fit with experimental results, as can be seen in Fig. 8 (all R<sup>2</sup>-values are attached). Therefore, the considered way of obtaining the FEM model proved to be satisfactory and is recommended by this research group for all future polymer simulations.

## CONCLUSIONS

This research includes three PLA specimen groups (100 % infill) with different layer heights (0.3, 0.2, and 0.1 mm), tested at 1 mm/min speed and afterwards at 10 mm/min. The 0.2 mm and 0.1 mm specimens have similar properties, with higher stiffness and UTS than 0.3 mm specimens, but lower overall strain. Higher loading speed increases stiffness and UTS but slightly decreases strain. The infill density effect was assessed by an additional set of 90 % specimens (1 mm/min) to patch and interpolate our data with 90-10 % results from /9/. In this way, the exhausting acquisition of 100 to 10 % infill data is bypassed, providing presentable results for our material.

The acquired data is then used to create precise PLA constitutive models in the MCalibration software, for all layer cases (100 % infill). The FEM models' accuracy is verified by comparing stress-strain outputs from the Abaqus CAE software with experimental data. By segmenting the data into smaller parts, the MCalibration could create precise material models with R<sup>2</sup>-value fit of 0.999, which are valuable for future, more complicated FEM analyses.

## ACKNOWLEDGEMENTS

The authors acknowledge the support from the Ministry of Science, Technological Development and Innovations of the Republic of Serbia, under contract No. 451-03-66/2024-03/200213 (from February 5, 2024).

## REFERENCES

- Milovanović, A., Milošević, M., Mladenović, G., et al. (2019), *Experimental dimensional accuracy analysis of reformer prototype model produced by FDM and SLA 3D printing technology*, In: Mitrović, N., Milošević, M., Mladenović, G. (Eds.) *Experimental and Numerical Investigations in Materials Science and Engineering*, CNNTech 2018. Lecture Notes in Networks and Systems (LNNS), vol.54. Springer, Cham.: 84-95. doi: 10.1007/978-3-319-99620-2\_7
- Milovanović, A., Sedmak, A., Grbović, A., et al. (2020), *Comparative analysis of printing parameters effect on mechanical properties of natural PLA and advanced PLA-X material*, *Procedia Struct. Integr.* 28(5): 1963-1968. doi: 10.1016/j.prostr.2020.11.019
- Petersmann, S., Spoerk, M., Van De Steene, W., et al. (2020), *Mechanical properties of polymeric implant materials produced by extrusion-based additive manufacturing*, *J Mech. Behav. Biomed. Mater.* 104: 103611. doi: 10.1016/j.jmbbm.2019.103611
- Farah, S., Anderson, D.G., Langer, R. (2016), *Physical and mechanical properties of PLA, and their functions in widespread applications - A comprehensive review*, *Adv. Drug Deliv. Rev.* 107: 367-392. doi: 10.1016/j.addr.2016.06.012

5. Jem, K.J., Tan, B. (2020), *The development and challenges of poly (lactic acid) and poly (glycolic acid)*, Adv. Ind. Eng. Polym. Res. 3(2): 60-70. doi: 10.1016/j.aiepr.2020.01.002
6. Castro-Aguirre, E., Iñiguez-Franco, F., Samsudin, H., et al. (2016), *Poly (lactic acid)-Mass production, processing, industrial applications, and end of life*, Adv. Drug Deliv. Rev. 107: 333-366. doi: 10.1016/j.addr.2016.03.010
7. Bajpai, P.K., Singh, I., Madaan, J. (2014), *Development and characterization of PLA-based green composites: A review*, J Thermopl. Compos. Mater. 27(1): 52-81. doi: 10.1177/0892705712439571
8. Tsuji, H. (2016), *Poly (lactic acid) stereocomplexes: A decade of progress*, Adv. Drug Deliv. Rev. 107: 97-135. doi: 10.1016/j.addr.2016.04.017
9. Pandzic, A., Hodzic, D., Milovanovic, A. (2019), *Effect of infill type and density on tensile properties of PLA material for FDM process*, In: B. Katalinic (Ed.) Proc. 30<sup>th</sup> DAAAM Int. Symp., DAAAM Int. Vienna, Austria, pp. 0545-0554. doi: 10.2507/30th.daaam.proceedings.074
10. Milovanović, A., Golubović, Z., Babinský, T., et al. (2022), *Tensile properties of polypropylene additively manufactured by FDM*, Struct. Integr. Life, 22(3): 305-308.
11. Milovanović, A., Golubović, Z., Kirin, S., et al. (2023), *Manufacturing parameter influence on FDM polypropylene tensile properties*. J Mech. Sci. Technol. 37(11): 5541-5547. doi: 10.1007/s12206-023-2305-5
12. Donate, R., Monzón, M., Alemán-Domínguez, M.E. (2020), *Additive manufacturing of PLA-based scaffolds intended for bone regeneration and strategies to improve their biological properties*, e-Polym. 20(1): 571-599. doi: 10.1515/epoly-2020-0046
13. Li, Y., Yuan, S., Zhang, W., Zhu, J. (2023), *A new continuous printing path planning method for gradient honeycomb infill structures*, Int. J Adv. Manuf. Technol. 126: 719-734. doi: 10.1007/s00170-023-11065-1
14. Milovanović, A., Golubović, Z., Trajković, I., et al. (2022), *Influence of printing parameters on the eligibility of plane-strain fracture toughness results for PLA polymer*, Procedia Struct. Integr. 41: 290-297. doi: 10.1016/j.prostr.2022.05.034
15. Milovanović, A., Milošević, M., Trajković, I., et al. (2022), *Crack path direction in plane-strain fracture toughness assessment tests of quasi-brittle PLA polymer and ductile PLA-X composite*, Procedia Struct. Integr. 42: 1376-1381. doi: 10.1016/j.prostr.2022.12.175
16. Epsilon Technology Corp. (n.d.). (last accessed April 17, 2024) <https://www.epsilontech.com/products/axial-extensometer-model-3542/>
17. Milovanović, A., Montanari, M., Golubović, Z., et al. (2024), *Compressive and flexural mechanical responses of components obtained through mSLA vat photopolymerization technology*, Theor. Appl. Fract. Mech. 131: 104406. doi: 10.1016/j.tafmec.2024.104406
18. Gates, T.S., Feldman, M. (1995), *Time-dependent behavior of a graphite/thermoplastic composite and the effects of stress and physical aging*, J Compos. Technol. Res. 17(1): 33-42. doi: 10.1520/CTR10511J
19. Ji, Q., Wang, Z., Yi, J., Tang, X. (2021), *Mechanical properties and a constitutive model of 3D-printed copper powder-filled PLA material*, Polymers, 13(20): 3605. doi: 10.3390/polym13203605
20. Hamel, S.E., Hermanson, J.C., Cramer, S.M. (2013), *Mechanical and time-dependent behavior of wood-plastic composites subjected to tension and compression*, J Thermopl. Compos. Mater. 26(7): 968-987. doi: 10.1177/0892705711432362
21. Bergström, J.S., Bischoff, J.E. (2010), *An advanced thermo-mechanical constitutive model for UHMWPE*, Int. J Struct. Changes Solids, 2(1): 31-39.

© 2024 The Author. Structural Integrity and Life, Published by DIVK (The Society for Structural Integrity and Life 'Prof. Dr Stojan Sedmak') (<http://divk.inovacionicentar.rs/divk/home.html>). This is an open access article distributed under the terms and conditions of the [Creative Commons Attribution-NonCommercial-NoDerivatives 4.0 International License](https://creativecommons.org/licenses/by-nc-nd/4.0/)